

$q = 4$ Potts model with Wolff cluster updates

Leia Barrowes

Phys 514 Final Project

December 3, 2020

1 Potts model Hamiltonian and order parameter

The Potts model [1] is a generalization of magnetization with q levels in place of the standard two. Each state has a label $S = 0, 1, \dots, q - 1$. The Hamiltonian defining the Potts model, Eq. (1.1) is a sum over neighboring sites j and k , which add a contribution of J when the neighbors have the same value, $S_j = S_k$.

$$H = -J \sum_{\langle jk \rangle} \delta(S_j, S_k) \quad (1.1)$$

In this model I take $J = k_B = 1$ for simplicity.

The order parameter m measures the amount of symmetry present in the system; $m = 0$ in a completely disordered state (site values are unpredictable), and $m = 1/q$ in a perfectly ordered state (all sites have the same value). There are several choices of m ; I used the definition shown in Eq. (1.2). An alternate definition is shown in Eq. (1.3). I found after testing that Eq. (1.2) gives smoother results, perhaps because it takes all numbers N_S into account rather than just one.

$$m = \left| \frac{1}{q} \sum_{S=0}^{q-1} \frac{N_S}{N} \exp \left(2\pi i \frac{S}{q} \right) \right| \quad (1.2)$$

$$m_{\text{alt}} = \frac{1}{q(q-1)} \left(q \frac{\max(N_0, N_1, \dots, N_{q-1})}{N} - 1 \right) \quad (1.3)$$

In this project I will take $q = 4$ and step through the thermalization process with the Wolff algorithm. I will analyze the second-order (continuous) phase transition that occurs at some critical temperature T_c [2]. A Potts system with $q > 4$ experiences first-order (discontinuous) phase transitions [3].

2 Wolff cluster update algorithm

The analysis is performed on a square lattice of length L with periodic boundary conditions. To initialize, a random integer between 0 and $q - 1$, each with equal probability, is assigned to each site. The system will reach thermal equilibrium through multiple iterations of the Wolff algorithm (I used $\gtrsim L^2 10^3$ iterations), a method that steps the system through configuration space.

The Wolff cluster update algorithm [4] makes local changes in the system by choosing a random site, building a cluster around it, then assigning a new single value to the entire cluster. The clusters are built from the initial site as follows:

- 1) Choose a random initial site.
- 2) If any neighboring site has the same value as the initial site, add it to the cluster with probability $1 - \exp(-\beta J)$.
- 3) Repeat step 2 for any added sites, being careful not to repeatedly add any sites for the sake of computational efficiency.



Figure 1: In this example ($k_B T/J = 2$, greater than the critical temperature), the bulk of the flipped cluster is in the bottom right corner of the lattice. Notice the site at the top that became part of the flipped cluster because the boundaries are periodic. Notice also that the site on the bottom, to the left of the flipped cluster, had the same initial value but did not join the cluster; remember, the probability of each site joining the cluster is less than 1.

4) Assign all the sites added to the cluster a new value between 0 and $q - 1$, not including the current value. Figure 1 shows an example of the result of one iteration of the above steps.

Most, if not all, papers reviewing the Wolff algorithm use probability $1 - \exp(-2\beta J)$ in step 2. These works likely model the Ising system and this probability does not apply to all systems. The most general expression is $1 - \exp[-\beta(\Delta E)_{\text{one flip}}]$, derived [5] from the Kandel-Domany framework [6] of configuration space exploration.

The Wolff algorithm is optimal for circumventing slow-down near the critical temperature because there are clusters of all sizes at criticality; flipping small clusters don't cost much computational effort, and flipping large clusters efficiently move the system through phase space. However, the algorithm is inefficient away from criticality because at low temperatures there is not much change per iteration, and at high temperatures there are no large clusters. The Swendsen-Wang algorithm [7] is more optimal for simulating non-critical systems because it identifies and flips every cluster in a system, each with probability $\frac{1}{2}$. The most efficient algorithms are a mix of these two techniques. Computational challenges specific to this project are detailed in Section 5.

3 Finding the critical temperature

The analytic result for the critical temperature [8] of the 2D Potts model is shown in Eq. (3.1).

$$T_c(q) = \frac{1}{\ln(1 + \sqrt{q})} \quad (3.1)$$

$$T_c(q = 4) = \frac{1}{\ln 3} \approx 0.910 \quad (3.2)$$

The most accurate way to measure the critical temperature T_c in the simulation (or in experiment) is through the Binder cumulant, shown in Eq. (3.3).

$$U_L(T) = 1 - \frac{\langle m(T)^4 \rangle}{3 \langle m(T)^2 \rangle^2} \quad (3.3)$$

$$U(T) = f \left(L^{1/\nu} (T - T_c) \right) \quad (3.4)$$

The Binder cumulant [9] as a function of temperature $U_L(T)$ has the same value at $T = T_c$ for any lattice size L ; therefore we find T_c by looking at the region of intersection of $U_L(T)$ for several different L . Before proceeding with finding the rest critical exponents, we can independently find the critical exponent ν , defined in Eq. (4.1). The master Binder cumulant U is a function of $L^{1/\nu}(T - T_c)$. Once I shift the independent axis to $t \equiv L^{1/\nu}(T - T_c)$, I can guess-and-check to find the ν that makes all the cumulant curves $U_L(t)$ overlap into the master curve $U(t)$ [10].

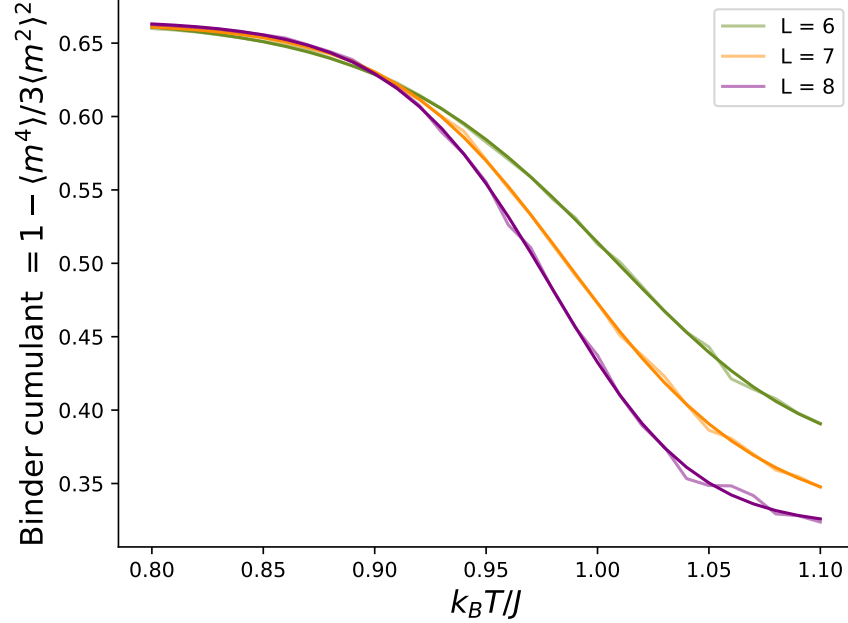


Figure 2: Binder cumulant data and general logistic fit for various lattice length L . The Binder cumulants $U_L(T)$ have a universal value at T_c for all L . Here, the three fitted curves intersect at $T_c \approx 0.905$.

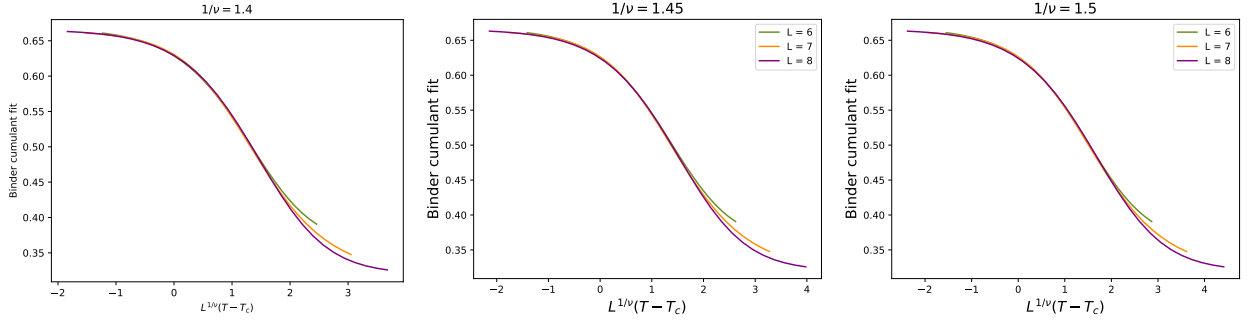


Figure 3: Binder cumulant general logistic fits, shifted by T_c and scaled by slightly different powers of L . This horizontal transformation should result in a master curve $U(t)$, considering this domain of $t \equiv L^{1/\nu}(T - T_c)$: $-2 < t < 2$. It's necessary to zoom in on the figures to see the following: for $1/\nu = 1.40$, the curves diverge as t approaches 2; for $1/\nu = 1.50$, the three curves start separating from each other in the domain $0 < t < 2$.

I find that my Binder cumulant curves, shown in Fig. 2, intersect at $T_c \approx 0.905$, a -0.58% difference from the analytic solution (Eq. (3.2)). Through the sort of guess-and-check bisection-like method with the temperature scaling, shown in Fig. 3, I find that $1/\nu = 1.45$; this is a 3.4% difference from the analytic value, $1/\nu = \frac{3}{2}$ [11].

4 Finding the critical exponents

The behavior of the specific heat, order parameter, and susceptibility are all be described by power laws near critical temperature because the phase transition is continuous. These power laws and associated exponents are defined in Eqs. (4.2) to (4.4).

Finding these critical exponents is easy because we independently found ν in Section 3. We can take

advantage of the finite size of these simulations: theoretically, the correlation length $\xi \rightarrow \infty$ as $T \rightarrow T_c$, as suggested in Eq. (4.1). However, in a finite system a diverging correlation length is impossible, and we instead have $\xi \sim L$ near critical temperature. Therefore, we can replace ξ in Eqs. (4.2) to (4.4) with L and find α , β , and γ by running simulations with various L keeping the temperature fixed at T_c .

$$\xi \propto |T_c - T|^{-\nu} \quad (4.1)$$

$$C \propto |T_c - T|^{-\alpha} \propto \xi^{\alpha/\nu} \quad (4.2)$$

$$m \propto (T_c - T)^\beta \propto \xi^{-\beta/\nu} \quad (4.3)$$

$$\chi \propto |T_c - T|^{-\gamma} \propto \xi^{\gamma/\nu} \quad (4.4)$$

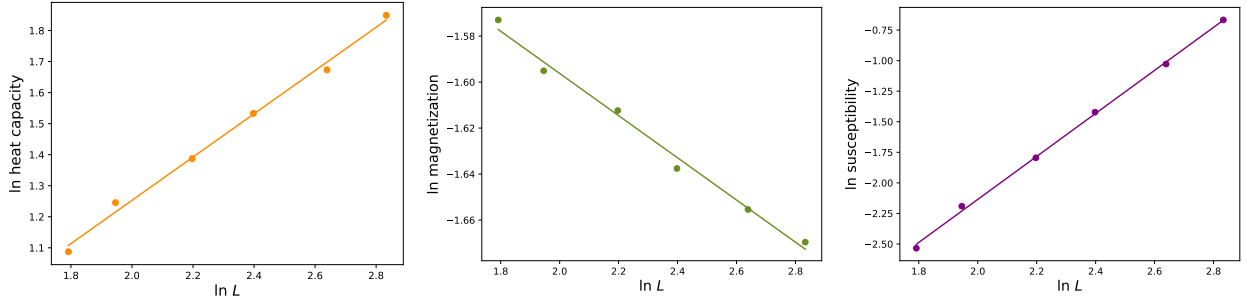


Figure 4: Log-log plots of various observables plotted versus lattice length L : heat capacity C , magnetization (order parameter) m , and susceptibility χ . Thanks to finite scaling, these plots have linear shapes on a log-log plot, with the slopes corresponding to the exponents on ξ in Eqs. (4.2) to (4.4). This linear behavior appears above some minimum L , which I found to be $L = 5$. Therefore, I used $L \geq 6$ throughout this project. Lower L s result in data points that curve away from the linear trend because small lattice sizes are too coarse-grained to show the true behavior of the phase transition.

From the slopes of these linear fits, I find that $\alpha = 0.481$, $\beta = 0.0633$, and $\gamma = 1.21$. The analytic values are $\alpha = 2/3$, $\beta = 1/12$, and $\gamma = 7/6$ [11], which are 24.1%, 27.9%, and -3.98% off different, respectively. The heat capacity and magnetization were very sensitive to the critical temperature; using the analytic critical temperature gave much more correct results, but these presented results are at least the correct order of magnitude and sign.

5 Computational challenges: accuracy VS speed

The main computational challenge is finding accurate results without too much computational cost, as is the challenge with most computing projects. As mentioned in Section 2, the Wolff algorithm is very efficient near T_c and inefficient away from criticality. Finding T_c is one of the objectives of this lab, so knowing the analytic solution for T_c is helpful for knowing where to search and for keeping simulation times low. Finding T_c requires three simulations, each with different lattice length L . However, the Potts model is inaccurate at low L . I can find the lower bound of accurate L s by running the second part of the project, where I find α , β , and γ . The data starts diverging a bit off-linear at low L (see Fig. 4). Before I find the exact right critical temperature, this process is slower than usual. In retrospect, I should have used the analytic T_c to find the minimum accurate L before finding my experimental T_c . Instead, I iteratively made each half of the project more accurate (Binder cumulant and exponent determination).

6 Conclusion and acknowledgements

An interesting future project would focus on characterizing the phase transition for general q , since analytic solutions exist for general q . I'd like to find real-life examples of the Potts model to make this work meaningful as well.

Huge thanks to Professor Gull for the lectures and patience with project help. Although it can be traced back to the main works cited, I learned most uncited information in this project from him.

References

- ¹R. Potts, “Some generalized order-disorder transformations”, *Proc. Cambridge Phil. Soc.* **48**, 106–109 (1952).
- ²H. Duminil-Copin, V. Sidoravicius, and V. Tassion, “Continuity of the Phase Transition for Planar Random-Cluster and Potts Models with $1 \leq q \leq 4$ ”, *Communications in Mathematical Physics* **349**, 47–107 (2016).
- ³H. Duminil-Copin, M. Gagnebin, M. Harel, I. Manolescu, and V. Tassion, *Discontinuity of the phase transition for the planar random-cluster and Potts models with $q > 4$* , 2017, [arXiv:1611.09877 \[math.PR\]](#).
- ⁴U. Wolff, “Collective Monte Carlo Updating for Spin Systems”, *Phys. Rev. Lett.* **62**, 361–364 (1989).
- ⁵G. T. Barkema and M. E. J. Newman, *New Monte Carlo algorithms for classical spin systems*, tech. rep. cond-mat/9703179. SFI-97-03-027 (1997).
- ⁶D. Kandel, E. Domany, and A. Brandt, “Simulations without critical slowing down: Ising and three-state Potts models”, *Phys. Rev. B* **40**, 330–344 (1989).
- ⁷R. H. Swendsen and J.-S. Wang, “Nonuniversal critical dynamics in Monte Carlo simulations”, *Phys. Rev. Lett.* **58**, 86–88 (1987).
- ⁸A. Boer, “Monte Carlo simulation of the two-dimensional Potts model using nonextensive statistics”, *Physica A: Statistical Mechanics and its Applications* **390**, 4203–4209 (2011).
- ⁹K. Binder, “Finite size scaling analysis of ising model block distribution functions”, *Zeitschrift fur Physik B Condensed Matter* **43**, 119–140 (1981).
- ¹⁰*ALPS 2 Tutorials:MC-07 Phase Transition*, http://alps.comp-phys.org/mediawiki/index.php/ALPS_2_Tutorials:MC-07_Phase_Transition.
- ¹¹R. J. Creswick and S.-Y. Kim, “Critical exponents of the four-state Potts model”, *Journal of Physics A: Mathematical and General* **30**, 8785–8786 (1997).
- ¹²J. Caldeira, W. Wu, B. Nord, C. Avestruz, S. Trivedi, and K. Story, “DeepCMB: Lensing reconstruction of the cosmic microwave background with deep neural networks”, *Astronomy and Computing* **28**, 100307 (2019).